Dielectric Spectroscopy of the Room Temperature Molten Salt Ethylammonium Nitrate

H. Weingärtner and A. Knocks

Physikalische Chemie II, Ruhr-Universität Bochum, D-44780 Bochum, Germany

W. Schrader and U. Kaatze*

Drittes Physikalisches Institut, Georg-August-Universität, Bürgerstrasse 42−44, D-37073 Göttingen, Germany

Received: April 18, 2001; In Final Form: June 17, 2001

The complex permittivity of ethylammonium nitrate has been measured as a function of frequency between 3 MHz and 40 GHz at eight temperatures between 288.15 and 353.15 K. The spectra are well represented by a sum of a conductivity term and a relaxation spectral function that reflects an unsymmetrical relaxation time distribution. Parameter values are given for the Cole−Davidson term and the Kohlrausch−Williams−Watts model. Molecular mechanisms in conformance with an unsymmetrical relaxation time distribution are discussed. The dominant relaxation process with a relaxation frequency in the accessible range can be explained by the formation of a small amount of dipolar ion complexes. The values for the extrapolated high-frequency permittivity indicate a further relaxation process, well above the frequency range of measurements, which is likely to reflect modes of motions of the cation and anion lattices relative to one another.

1. Introduction

Dielectric spectroscopy is one of the oldest techniques for studying dynamical processes in liquids[1] and has frequently been applied for monitoring dynamical phenomena in electrolyte solutions.[2−5] Here, we extend such measurements to fluid molten salts of high electrical conductivity by studying dielectric behavior of the room temperature fused salt ethylammonium nitrate (EAN) from the melting point at 287 K to 353 K. In the context of designing new classes of solvents, room temperature molten salts have recently become of major interest.[6]

EAN has occasionally been used as a solute[7] or solvent[8] in solution chemistry. Its viscosity (35 cP at 25 °C)[9] is typical for many molten salts with low melting points.[10] The electrical conductivity[9] indicates the quite high dissociation. Nevertheless, one expects some association due to hydrogen bonds between the ethylammonium cations and the nitrate ions.[7−9] It has been argued[11] that these hydrogen bonds are capable of inducing a network structure which in some respects mimics the three-dimensional hydrogen-bonded network of water.

Dielectric spectroscopy of fused salts in the fluid region is an almost untouched field. The available work is limited to highly viscous systems near their glass transition.[12] Results for more fluid systems include data for mixtures of $Ca(NO_3)_2$ and KNO_3[13] and the highly viscous room temperature fused salt tri-*n*-octylmethylammonium chloride.[14] Morabin and Tete[15] have reported on the permittivity of molten alkali metal nitrates near 600 K at a frequency near 10 Hz, taken as a measure for the static permittivity of such systems.

Theoretical work on the dielectric behavior of molten salts is scarce as well. Doucet et al.[16] have developed a framework for treating the dielectric polarization of molten salts, but no working equations were derived. Some theoretical scenarios come from work on concentrated electrolyte solutions[3] and on relaxation processes in ionic glasses and supercooled liquids.[12,17,18] Before developing more adequate theories for dielectric relaxation in fluid molten salts, a detailed experimental characterization seems mandatory.

2. Experimental Section

We have measured the complex permittivity of a liquid sample of EAN (melting point 287.3 K) which was synthesized and dried as described elsewhere.[7] The measurements were performed at frequencies $\nu = \omega/2\pi$ in the range between 3 MHz and 40 GHz and at temperatures between 288 and 353 K. The complex relative permittivity $\epsilon^*(\nu)$ is given as[1] ($i^2 = -1$)

$$\epsilon^*(\nu) = \epsilon'(\nu) - i\epsilon''(\nu) = \epsilon_\infty + \Delta\epsilon^*(\nu) + \sigma/i\epsilon_0\omega \quad (1)$$

ϵ_∞ is the high-frequency limit of the real part, associated with electronic and atomic displacement polarizations, and $\Delta\epsilon^*(\nu) = \epsilon^*(\nu) - \epsilon_\infty$ is the frequency-dependent part of the complex permittivity. The static permittivity (dielectric constant) ϵ_s is defined as the zero-frequency limit of the real part, i.e., $\epsilon_s \equiv \epsilon'(\nu\rightarrow 0) = \epsilon_\infty + \Delta\epsilon'(\nu\rightarrow 0)$. For conductive systems the imaginary part shows a divergent low-frequency response proportional to $\sigma/i\epsilon_0\omega$, where σ is the static (dc) conductivity and ϵ_0 denotes the electrical field constant.

Depending on the frequency range, the dielectric spectra were recorded by four different techniques. All methods yield data triples $\{\epsilon', \epsilon'', \nu\}$ of the real (ϵ') and imaginary (ϵ'') parts of the complex permittivity $\epsilon^* = \epsilon' - i\epsilon''$ at the frequency ν. At low frequencies, 3 MHz $< \nu <$ 3 GHz, input impedance measurements were performed at Göttingen using a special sample cell of the cutoff variety and a network analyzer system.[19] In the intermediate frequency range two techniques were employed. The method employed in Bochum at $1 < \nu < 20$ GHz is based on the analysis of reflected waves.[20] A second technique applied in Göttingen at $5.3 < \nu < 18$ GHz is based on a travelling wave method. The wave transmitted through liquid-filled circular waveguides was balanced against a reference wave, and the interferometer signal was automatically recorded at varying sample length.[21] From 18 to 40 GHz manually operated microwave bridges consisting of standard waveguide devices were used.[22]

The experimental error in complex permittivity data depends on the frequency and the method of measurement. In addition,

10.1021/jp0114586 CCC: $20.00
Published on Web 08/17/2001

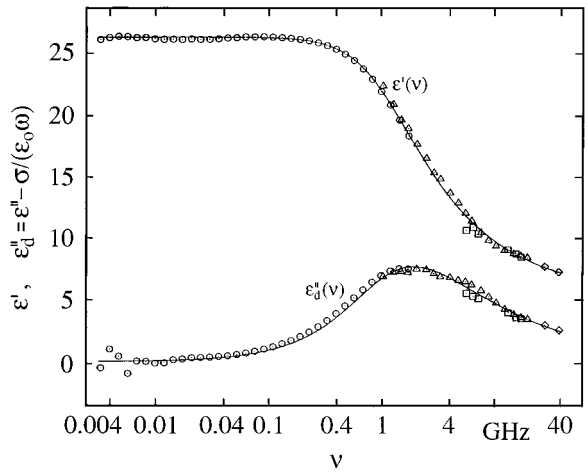

Figure 1. Real part and negative imaginary part, excluding conductivity contributions, of the complex permittivity spectrum of ethylammonium nitrate at 298.15 K. Figure symbols indicate different methods of measurements. The curves are graphs of the Cole−Davidson relaxation spectral function with the parameter values given in Table 1.

there are specific experimental difficulties in measurements with highly conductive media, where the sample is largely short-circuited by its high intrinsic conductivity. Because we employed different methods of measurements and different specimen cells, systematic errors are unlikely to be unnoticed. For the total permittivity ϵ^*, for most of the frequency range, the errors are ± 0.5 for both the real and the imaginary part. At low frequencies, where the conductivity contribution dominates ($\sigma/(\epsilon_0\omega) = 2 \times 10^4$ at 4 MHz and 298.15 K), the error is somewhat larger. Hence also larger is the error in the remaining dielectric contribution $\epsilon_d'' = \epsilon'' - \sigma/(\epsilon_0\omega)$ of the negative imaginary part of the permittivity after subtraction of the conductivity contribution (± 2, Figure 1).

3. Results

Permittivity Spectra. As a typical example of permittivity spectra, Figure 1 shows results for the measured ϵ' and ϵ'' data at 298.15 K as a function of frequency. For simplicity, $\epsilon''(\omega)$ is corrected for the conductivity term. The data for $\epsilon'(\nu)$ and $\epsilon''(\nu)$ were simultaneously parametrized, treating the static conductivity σ as an adjustable parameter. Several relaxation spectral functions $S^*(\nu) = S'(\nu) - S''(\nu)$ were examined. These functions were fitted to the measured data using a nonlinear Marquardt algorithm[23] to minimize the reduced variance:

$$\chi^2 = \frac{1}{N-P-1}\sum_{n=1}^{N}\left[\left(\frac{S'(\nu_n)-\epsilon'(\nu_n)}{\delta\epsilon''(\nu_n)}\right)^2 + \left(\frac{S''(\nu_n)-\epsilon''(\nu_n)}{\delta\epsilon''(\nu_n)}\right)^2\right] \quad (2)$$

Herein ν_n ($n = 1, ..., N$) denotes the frequencies of measurement, P is the number of adjustable parameters of the model relaxation function S^*, and the inverse experimental errors $1/\delta\epsilon'(\nu_n)$ and $1/\delta\epsilon''(\nu_n)$ are used as weighing factors.

For parametrization we applied various relaxation models. We used a Havriliak−Negami[24] (HN) spectral function, defined as

$$\Delta\epsilon^* = \frac{\epsilon_s - \epsilon_\infty}{(1 + (i\omega\tau_{HN})^{1-\alpha})^\beta} \qquad 0 \le \alpha < 1,\ 0 < \beta \le 1 \quad (3)$$

which includes as limiting forms the Debye relaxation term (D, $\alpha = 0$, $\beta = 1$),[25] the Cole−Cole term[26] (CC, $\beta = 1$), and the Cole−Davidson term[27] (CD, $\alpha = 0$). It was found that the CD term, which presumes an unsymmetrical relaxation time distribution, nicely applies for the measured spectra (Figure 1). The need for an unsymmetrical distribution function is obvious from the asymmetric shape of the measured $\epsilon_d''(\nu)$ in Figure 1. The pulse-response function belonging to the CD spectral function is given by ($\tau_{CD} = \tau_{HN}$)[28]

$$f_{CD}(t) = \frac{1}{\tau_{CD}\Gamma(\beta)}\left(\frac{t}{\tau_{CD}}\right)^{\beta-1}\exp(-t/\tau_{CD}) \quad (4)$$

with Γ denoting the Gamma function. The parameters found for the CD relaxation spectral function are collected in Table 1.

A double Debye term model turned out to be less appropriate for the present spectra. A satisfactory description of the measured permittivity data was, however, obtained with the Hill[29] (H) relaxation term, which is defined by the negative imaginary part:

$$\Delta\epsilon'' = \frac{\epsilon_s - \epsilon_\infty}{(1 + (\omega\tau_H)^{2s})^{(m+n)/2s}} \quad (5)$$

The parameters m, n, and s ($0 < m, n, s \le 1$) determine the shape and width of the relaxation time distribution. Since the real part of the Hill spectral function is not available analytically, it was calculated numerically, utilizing the Kramers−Kronig relations. The low-frequency branch of the Hill term is determined by the parameter m. We found that choosing $m = 1$ well represents this branch, which implies that at low frequencies the spectral function resembles a Debye term. Correspondingly, we fixed this parameter at $m \equiv 1$ in all fits.

Another suitable relaxation function is based upon the Kohlrausch−Williams−Watts approach[30] (KWW), for which the pulse response function is defined as

$$f_{KWW}(t) = \frac{p}{\tau_{KWW}}\left(\frac{t}{\tau_{KWW}}\right)^{p-1}\exp[-(t/\tau_{KWW})^p] = -\,\mathrm{d}\Phi(t)/\mathrm{d}t \quad (6)$$

with the dielectric decay function $\Phi(t)$ given by a stretched exponential

$$\Phi(t) = \exp[-(t/\tau_{KWW})^p] \quad (7)$$

The KWW spectral function was calculated numerically from the pulse response function as

$$\Delta\epsilon^*(\nu) = (\epsilon_s - \epsilon_\infty)\int_0^\infty \exp(-i\omega t)[f_{KWW}(t)]\,\mathrm{d}t \quad (8)$$

The description of the measured spectra by the KWW function yielded practically the same reduced variance (eq 2) in the fits as that by the CD function; e.g., at 25 °C χ^2(KWW) = 0.079 and χ^2(CD) = 0.082, whereas at 35 °C χ^2(KWW) = 0.071 and χ^2(CD) = 0.065. Hence from the deviations of the experimental data from the analytical expressions, preference for either of the two relaxation spectral functions over the other one is impossible. The parameters of the KWW model are thus also given in Table 1.

Auxiliary Data. Table 1 includes a series of auxiliary data: (1) Static conductivities σ were extracted from the dielectric spectra. (2) Molar conductances $\Lambda = \sigma/C$, where C is the molar concentration, were determined from the conductivities and from density data measured pycnometrically. (3) Shear viscosities η

TABLE 1: Parameters Describing the Complex Permittivity of EAN and Some Auxiliary Quantities for Data Evaluation

	T/K					
	288.15	298.15	308.15	318.15	338.15	353.15
c/(mol·L^{-1}) ± 0.1%	11.26	11.21	11.14	11.10	10.99	10.90
d/(g cm^{-3}) ± 0.1%	1.218	1.212	1.205	1.200	1.189	1.179
σ/(S cm^{-1}) ± 10%	0.024	0.028	0.033	0.039	0.047	0.061
Λ/(S cm^{-2}/mol) ± 10%	2.12	2.52	2.95	3.51	4.34	5.63
η/cP ± 2%	50.00	34.88	25.67	19.28		
n_D ± 0.5%	1.453	1.450	1.447	1.444	1.442	1.439
ϵ_s(CD) ± 2%	27.1	26.2	25.1	23.6	23.3	22.2
ϵ_s(KWW) ± 2%	27.8	26.3	25.1	23.7	23.7	22.4
ϵ_∞(CD) ± 10%	4.2	4.8	4.4	4.5	4.6	4.8
ϵ_∞(KWW) ± 10%	5.5	6.0	5.8	5.9	6.0	6.0
τ_{CD}/ps ± 5%	179	140	127	103	69	60
τ_{KWW}/ps ± 5%	78	64	55	44	33	28
β ± 10%	0.50	0.52	0.49	0.48	0.50	0.50
p ± 10%	0.69	0.71	0.70	0.70	0.71	0.72

TABLE 2: Arrhenius Parameters for the Static Molar Conductance, Shear Viscosity, and Relaxation Times of the CD and KWW Fits

	X_0	E_X/(kJ mol^{-1})
Λ	366 S cm^{-2} mol^{-1}	12.4
η	0.0018 cP	24.5
τ_{CD}	0.45 ps	14.4
τ_{KWW}	0.25 ps	13.7

were measured by a falling-ball viscometer. (4) Refractive indices n_D were measured at the wavelength of the sodium D line using a standard refractometer. At 298.15 K our results differ markedly from previously reported conductance[7,9] and viscosity[31,32] data. We attribute the difference to uncontrollable traces of water in the samples used earlier.

4. Discussion

Electrical Conductivity and Viscosity. In the limited temperature range considered here, the simple Arrhenius expression

$$X = X_0 \exp(E_X/RT) \qquad X = \eta,\ 1/\Lambda,\ \tau_{CD},\ \tau_{KWW} \tag{9}$$

proved to be sufficient to represent the temperature dependence of the viscosity and electrical conductance. The activation energies E_X and preexponential factors X_0 are given in Table 2. The activation energy for the viscosity is substantially larger than that for the molar conductivity, which is typical for many other molten salts.[10] The conductance-viscosity ("Walden") products of EAN, $NaNO_3$, and KNO_3 are roughly of the same order of magnitude.

In total, our conductance and viscosity data for EAN are not substantially different from what is obtained with the alkali metal nitrates. This implies that EAN possesses a quite high ionicity with some ion pairs present, as found with alkali metal nitrates as well.[10] We know from work on solutions of EAN in solvents of low polarity[7] that ion pairing is substantially larger than for comparable quaternary ammonium salts without residual protons. Similar observations are were made for other ammonium salts.[33] This enhanced ion pairing is attributed to hydrogen bonds between the residual protons of the cation and proton-accepting anions. Such hydrogen bonds are also believed to exist in the pure salt.[11] At present, there is no clear evidence for effects of such hydrogen bonds upon the conductance.

Extrapolated High-Frequency Permittivity. We turn now to results for the complex permittivity. As already noted, only asymmetrical distributions of relaxation times led to satisfactory description of the dielectric spectra. Specifically, we consider here the CD and KWW representations. The complete HN equation generalizes the CD expression by a further adjustable parameter, but only a marginal improvement of the data representation was found. Thus, we do not consider the HN representation in detail. For the same reason, the Hill spectral function is not explicitly used in the following.

All these relaxation functions do not satisfy a rigorous physical constraint

$$\lim_{\nu\to\infty} d\epsilon''(\nu)/d\epsilon'(\nu) = -\infty \tag{10}$$

for the high-frequency limit[34] of the spectral function. In the absence of more complete models, we nevertheless used these empirical relaxation functions for high-frequency extrapolation of the spectra.

Due to their obvious incompleteness, the extrapolated permittivity values ϵ_∞ differ markedly in the CD and KWW fits (Table 1). The figures from both fits are however substantially higher than $n^2 \approx 2.1$ as estimated from the refractive index in Table 1. There must exist at least one additional process at frequencies beyond the range considered here. Within experimental uncertainty the dispersion step $\epsilon_\infty - n^2$ is independent of temperature.

According to Ngai,[35] data in the mega- and gigahertz range for a variety of ionic conductors in the supercooled, glassy, or solid state yield extrapolated high-frequency permittivities on the order of $\epsilon_\infty \cong 8$, indicating an additional regime of dielectric dispersion and loss at very high frequencies. Ngai presents some evidence, for instance by analyzing neutron scattering data, that this additional contribution is associated with vibrational motions of the ions. It is thus an obvious attempt to relate the dispersion step $\epsilon_\infty - n^2$, at least in part, to the motions of the cation lattice with respect to that of the anions, in analogy with lattice dynamics theories for ferroelectrics.[36]

On the other hand, there is an alternative scenario for this high-frequency contribution. In water[37−40] and alcohols[41,42] there seems to be a regime of dielectric loss at high frequencies, possibly associated with the suggested lifetime of a hydrogen bond.[43] Irrespective of the fact that alternative explanations for this contribution are presently discussed,[37,41,42] one may argue that a similar process may also contribute to the high-frequency permittivity of hydrogen-bonded EAN. Both explanations for the high-frequency mode imply that this mode is not intrinsically coupled to the primary relaxation process at lower frequencies.

Turning to the relaxation parameters, the relaxation time distributions are comparatively broad. Within experimental uncertainty, the width of the CD distribution is characterized by parameter $\beta = 0.5$, which shows no detectable temperature dependence. In terms of the KWW distribution, the observed width, $p \cong 0.70$, is independent of temperature as well. Both the relaxation times τ_{CD} and τ_{KWW} exhibit an Arrhenius-type

temperature dependence with practically the same activation energies (Table 2). The activation energies are roughly on the same order of magnitude as that of the static conductance, but substantially lower than that of the viscosity.

Extrapolated Static Permittivity. As the measurements have been conducted down to sufficiently low frequencies ν_{min} ,$\nu_{min} \cong 10^{-3}(2\pi\tau_{KWW})^{-1}$, the ϵ_s values are well-defined by the frequency-dependent complex permittivity data. Therefore, the ϵ_s values from the fits of the CD and KWW functions agree within the limits of experimental error (Table 1). The ϵ_s values decrease markedly with temperature T.

Data for a mixture of 40% $Ca(NO_3)_2$ + 60% KNO_3[10,12] show one relaxation term which extrapolates to $\epsilon_s \cong 20$, presumably due to configurations involving K^+ ions. Data for alkali metal nitrates imply $\nu \cong 10$ GHz. Morabin and Tete have reported $\epsilon'(10\ \text{GHz}) \cong 20$.[15] While the differing conditions do not permit a detailed comparison with our results, these figures are fairly consistent with what is observed by us.

Note that, in contrast to Na^+ or K^+, the $C_2H_5NH_3^+$ cation possesses a nonvanishing electrical dipole moment μ_{cation}. Using the Kirkwood−Fröhlich theory[44] for the static permittivity of a one-component dipolar liquid

$$\epsilon_s - \epsilon_\infty = \frac{N_A}{k_B T \epsilon_0} \frac{\epsilon_s}{2\epsilon_s + \epsilon_\infty} g c_\mu \mu^2 \qquad (11)$$

$\mu = \mu_{cation}$ can be estimated from the extrapolated static and high-frequency permittivity values and from the dipole concentration c_μ. In eq 11 N_A is Avogadro's number, k_B is the Boltzmann constant, g is the Kirkwood orientation correlation factor,[45] c_μ denotes the concentration, and μ is the dipole moment of the dipolar species in the liquid. With $g = 1$ one finds $\mu_{cation} = 2$ D, which is by far larger than expected for the fairly symmetrical ethylammonium ion.

An intriguing mechanism that might, however, contribute to the static permittivity ϵ_s of the molten salt is the formation of dipolar ion complexes. If these complexes are sufficiently long-lived, their thermally activated hindered motions result in a dielectric relaxation process as usually encountered in nonconducting dipolar fluids. For simplicity let us assume an ion pair equilibrium

$$C_2H_5N^+H_3 + NO_3^- \leftrightarrow C_2H_5N^+H_3 \cdot NO_3^-$$

with the forward (k_f) and reverse (k_r) rate constants and the equilibrium constant $K = k_f/k_r$. Estimating the distance between the cationic and the anionic charge of the ion as 0.34 nm, the electric dipole moment of the ion pair is $\mu = 0.54 \times 10^{-28}$ Asm = 16.3 D within the polarizable liquid.

Let us use this upper limit to estimate a lower limit of the ion pair association constant needed to rationalize the observed dielectric constant. Applying eq 11 analogously shows that at 298.15 K a concentration of $c_\mu = 1$ mol/L of the dipolar ion pairs is necessary in order to account for the extrapolated static permittivity ϵ_s. The EAN concentration is about 11 mol/L (Table 1). Hence the small fraction of 0.08 of the ions, forming contact ion pairs with lifetimes equal to or larger than the dielectric relaxation time, is sufficient to explain the comparatively high extrapolated low-frequency permittivity. This ion pair concentration corresponds to an equilibrium constant $K = 0.007$. If such model of ion pair formation is accepted, still about 92% of the ions may contribute to the dc conductivity of the molten salt. This is well in accordance with the conductance data reported earlier.

Relaxation Time Distribution. There is at least one theory which may explain the distribution of relaxation times by a dipolar scenario. In Glarum's defect diffusion model[46] a dipole relaxes instantaneously upon arrival of a diffusing defect. Glarum's ideas are built into a one-dimensional model, but were later generalized to three dimensions by Hunt and Powles,[47] Bordewijk,[48] and Cachet et al.[49] The latter work was specifically designed to describe ion pair relaxation in electrolyte solutions. All models end up with an unsymmetrical distribution of relaxation times. Specifically, Glarum's original model involves a relaxation time τ_r for the rotational diffusion of the dipolar species and another time constant τ_d characteristic for the diffusion of defects. If both times are equal, the dielectric relaxation follows a CD distribution with $\beta = 0.5$ and with $\tau_r = \tau_d$ being the principal relaxation time. In fact, our spectra can be well represented by a CD relaxation time distribution with $\beta = 0.5$ (Table 1).

Refined theories yield more complex expressions, although the same qualitative behavior. If τ_r is significantly larger than τ_d, the model of Bordewijk[48] and also the extension of Glarum's ideas to diffusion into three dimensions[52] result in a KWW distribution function with $p = 0.5$ somewhat different from $p = 0.7$ resulting from the analysis of our spectra. Under certain conditions the model of molecular reorientation in a fluctuating environment by Anderson and Ullmann[50] predicts also an unsymmetrical relaxation time distribution. Again two characteristic time constants have to almost coincide to yield the unsymmetrical distribution, namely the reorientation time τ_r and the structure relaxation time τ_s, the autocorrelation time of the density fluctuations. Hence the existence of an unsymmetrical distribution of relaxation times is well in accordance with a mechanism based on dipolar ion pair reorientation. Since both the CD and the KWW model are suited to describe the experimental spectra within the limits of experimental error (and with almost identical variance), no clear-cut conclusion can be drawn presently on the underlying relaxation mechanism.

Though it is an obvious attempt to explain the complex permittivity spectra of the EAN system by ion complexes, we are aware of possible alternative mechanisms. The Debye−Falkenhagen (DF) theory of dielectric relaxation in dilute electrolyte solutions[51] implies that the free ions can themselves give rise to a polarization without the existence of specific dipolar complexes. In the DF theory the contribution to the dielectric spectrum reflects the deformation of ionic atmospheres. This contribution is superimposed on the steady motion of the ions which gives rise to the static current. While DF theory applies at ion densities and conditions far away from those considered here, there have been attempts to generalize the DF idea. For instance, Badiali et al.[3,52] have started from the assumption that the ions were moving by Brownian linear motion, interrupted by collisions with other particles. Their result points toward a bimodal distribution, and could fit the data of many electrolyte solutions in apolar solvents at quite high salt concentrations.[3] On the other hand, Farber and Petrucci[53] have noted that the same data could be rationalized by the presence of ion pairs without resorting to DF-type ionic contributions. Badiali's theory is not specifically bound to the presence of a solvent, and may thus apply qualitatively to molten salts as well. A bimodal distribution is compatible with our findings only when the high-frequency relaxation mode is directly coupled to the primary relaxation process. Modeling shows, however, that at least the wing of the high-frequency mode of Badiali's theory must fall into the frequency range covered by us. Thus, in the specific form, this theory is not confirmed by our data.

Funke and Riess[17] have developed a jump relaxation model for glassy and solid conductors which, in parts, adapts the DF idea. In their model an ion jumps from a structurally relaxed position to a new position of higher potential energy. Subsequently, the ion may move back to the original position, or the structure of the surrounding ions may relax. Only in the latter case is a contribution to the static conductance obtained. The theory by Funke and Riess describes the major experimental features of conductivity relaxation in glasses. Attempts have been made to extend the theory to melts.

The theory rationalizes some essential features observed for EAN, although quantitative predictions are difficult. Funke's model is consistent with the stretched exponential behavior of the relaxation function predicted by KWW behavior.[54] In fact, in many glassy and solid conductors KWW behavior with an exponent of about $p = 0.65-0.68$ is found. This feature was first pointed out by Jonscher,[55] who denoted it as the "universal dielectric response". The exponent $p = 0.70$ found by us is very close to Jonscher's universal value. If the latter explanation provides the correct model, it is noteworthy that the KWW behavior is not specific to glassy and solid conductors, but represents an intriguing feature of ionic conductors in the fluid regime as well.

5. Conclusions

The microwave dielectric spectrum of the room temperature molten salt ethylammonium nitrate exhibits relaxation characteristics reflecting an underlying unsymmetrical relaxation time distribution. This relaxation term can be explained assuming the small amount of about 8% of the ions to form contact ion pairs with lifetimes larger than the dielectric relaxation time, which is on the order of 10^{-10} s (25 °C). Because of the comparatively large extrapolated high-frequency permittivity values ϵ_∞ ($n^2 + 2.1 \leq \epsilon_\infty \leq n^2 + 3.9$), motions of the cation and anion lattices relative to one another are likely to contribute to the complex permittivity spectrum at frequencies above the microwave region covered by our measurements.

Acknowledgment. Financial support of the Deutsche Forschungsgemeinschaft is gratefully acknowledged. Prof. R. Pottel is thanked for much spirited discussion.

References and Notes

(1) Hill, N. E.; Vaughan, W. E.; Price, A. H.; Davies, M. *Dielectric Properties and Molecular Behaviour*; Van Nostrand Reinhold: London, 1969.
(2) Pottel, R. In *Water. A Comprehensive Treatise*; Franks, F., Ed.; Plenum: New York, 1973; Vol. 3.
(3) Lestrade, J.-C.; Badiali J.-P.; Cachet, H. In *Dielectric and Related Molecular Processes* (*Specialist Periodical Reports*); Davies, M., Ed.; The Chemical Society: London, 1975; Vol. 2, p 106.
(4) Barthel, J. M. G.; Krienke H.; Kunz, W. *Physical Chemistry of Electrolyte Solutions. Modern Aspects;* Steinkopff: Darmstadt, 1998.
(5) Kaatze, U. *J. Solution Chem.* **1997**, *26*, 1049.
(6) Wasserscheid, P.; Keim W. *Angew. Chem., Int. Ed.* **2000**, *39*, 3773.
(7) Weingärtner, H.; Merkel, T.; Käshammer, S.; Schröer, W.; Wiegand, S. *Ber. Bunsen-Ges. Phys. Chem.* **1993**, *97*, 970.
(8) Mirejovsky, D.; Arnett, E. M. *J. Am. Chem. Soc.* **1983**, *105*, 1112.
(9) Benhlima, N.; Turmine, M.; Lettelier, P.; Naejus, R.; Lemordant, D. *J. Chim. Phys.-Phys. Chim. Biol.* **1998**, *95*, 25.
(10) Moynihan, C. T. In *Ionic Interactions. From Dilute Solutions to Fused Salts*; Petrucci, S., Ed.; Academic Press: New York, 1971; Vol. 1, Chapter 5, p 262.
(11) Evans, D. F.; Yamauchi, A.; Roman, R.; Casassa, E. Z. *J. Colloid Interface Sci.* **1982**, *86*, 89.
(12) Angell, C. A. *Chem. Rev.* **1990**, *90*, 523.
(13) Funke, K.; Hermeling, J.; Kumpers, J. *Z. Naturforsch. A* **1988**, *43*, 1094.
(14) Elsebrock, R.; Stockhausen, M.; Czechowski, G.; Jadzyn, J. *Pol. J. Chem.* **1998**, *72*, 2463.
(15) Morabin, Y. A.; Tete, A. *Rev. Gen. Electr.* **1968**, *77*, 961.
(16) Doucet, Y.; Gimenez, G.; Santini R.; Tete, A. *J. Chim. Phys.-Phys. Chim. Biol.* **1972**, *69*, 1761.
(17) Funke, K.; Riess, I. *Z. Phys. Chem., Neue Folge* **1984**, *140*, 217.
(18) Funke, K. *Z. Phys. Chem., Neue Folge* **1987**, *154*, 251.
(19) Göttmann, O.; Kaatze, U.; Petong,, P. *Meas. Sci. Technol.* **1996**, *7*, 525.
(20) Weingärtner, H.; Nadolny, H.; Volmari, A. *Ber. Bunsen-Ges. Phys. Chem.* **1998**, *102*, 866.
(21) Kaatze, U.; Pottel, R.; Wallusch, A. *Meas. Sci. Technol.* **1995**, *6*, 1201.
(22) Kaatze, U.; Giese, K. *J. Mol. Liq.* **1987**, *36*, 15.
(23) Marquardt, D. W. *J. Soc. Indust. Appl. Math.* **1963**, *2*, 2.
(24) Havriliak, S.; Negami, S. *J. Polym. Sci.* **1966**, *C14*, 99.
(25) Debye, P. *Polare Molekeln*; Hirzel: Leipzig, 1929.
(26) Cole, K. S.; Cole, R. H. *J. Chem. Phys.* **1941**, *9*, 341.
(27) Davidson, D. W.; Cole, R. H. *J. Chem. Phys.* **1950**, *18*, 1417.
(28) Davidson, D. W. *Can. J. Chem.* **1961**, *39*, 571.
(29) Hill, R. M. *Nature* **1978**, *275*, 96.
(30) Williams, G.; Watts, D. C. *Trans. Faraday Soc.* **1970**, *66*, 80.
(31) Poole, C. F.; Kersten, B. R.; Ho, S. S. J.; Coddens, M. E.; Furton, K. G. *J. Chromatogr.* **1986**, *352*, 407.
(32) Shetty, P. H.; Youngberg, P. J.; Kersten, B. R.; Poole, C. F. *J. Chromatogr.* **1987**, *411*, 61.
(33) Kraus, C. A. *J. Phys. Chem.* **1956**, *60*, 129.
(34) Powles, J. G. *J. Mol. Liq.* **1993**, *56*, 35.
(35) Ngai, K. L. *J. Chem. Phys.* **1999**, *110*, 10576.
(36) Fatuzzo, E.; Merz, W. E. *Ferroelectricity*; North-Holland: Amsterdam, 1967.
(37) Petong, P.; Pottel, R.; Kaatze, U. *J. Phys. Chem. A* **2000**, *104*, 7420.
(38) Afsar, M. N.; Hasted, J. B. *J. Opt. Soc. Am.* **1977**, *67*, 902.
(39) Ronne, C.; Thrane, L.; Astrand, P.-O.; Wallqvist, K A.; von Mikkelsen, A.; Keiding, S. R. *J. Chem. Phys.* **1997**, *107*, 5319.
(40) Ronne, C.; Astrand, P.-O.; Keiding, S. R. *Phys. Rev. Lett.* **1999**, *82*, 2888.
(41) Barthel, J.; Bachhuber, K.; Buchner, R.; Hetzenauer, H. *Chem. Phys. Lett.* **1990**, *165*, 369.
(42) Petong, P.; Pottel, R.; Kaatze, U. *J. Phys. Chem. A* **1999**, *103*, 6114.
(43) Ohmine, I.; Tanaka, H.; Wolynes, P. G. *J. Chem. Phys.* **1988**, *89*, 5852.
(44) Fröhlich, H. *Theory of Dielectrics*; Clarendon: Oxford, 1958.
(45) Kirkwood, J. G. *J. Chem. Phys.* **1939**, *7*, 911.
(46) Glarum, S. H. *J. Chem. Phys.* **1960**, *33*, 639.
(47) Hunt, B. I.; Powles, J. G. *Proc. Phys. Soc.* **1966**, *88*, 513.
(48) Bordewijk, P. *Chem. Phys. Lett.* **1975**, *32*, 952.
(49) Cachet, H.; Cyrot, A.; Fekir, M.; Lestrade, J. C. *J. Phys. Chem.* **1979**, *83*, 2419.
(50) Anderson, J. E.; Ullmann, R. *J. Chem. Phys.* **1967**, *47*, 2178.
(51) Debye, P.; Falkenhagen, H. *Phys. Z.* **1928**, *29*, 121.
(52) Badiali, J. P.; Cachet, H.; Lestrade, J. C. *Ber. Bunsen-Ges. Phys. Chem.* **1971**, *75*, 297.
(53) Farber, H.; Petrucci, S. *J. Phys. Chem.* **1975**, *79*, 1221.
(54) Funke, K.; Hoppe, R. *Solid State Ionics* **1990**, *40/41*, 200.
(55) Jonscher, A. K. *Nature* **1975**, *253*, 717.